Mon. Not. R. astr. Soc. (1981) **195**, 1011–1028

Catastrophic cooling in supernova remnants

S. A. E. G. Falle *Department of Applied Mathematical Studies, University of Leeds, Leeds LS2 9JT*

Received 1980 October 31; in original form 1980 September 9

Summary. The transition from the adiabatic (Sedov) phase of a spherically symmetric supernova remnant is studied numerically. The input physics is kept as simple as possible, but the interstellar magnetic field is included. It is shown that, for sufficiently large values of the explosion energy and ambient density, multiple shocks are formed. These shocks continue to be formed until the expansion velocity of the remnant falls below 108 km s^{-1}.

The X-ray luminosity of the remnant is also calculated and it is found that the mean X-ray temperature does not correlate with the expansion velocity once radiative cooling becomes important.

1 Introduction

In recent years there has been considerable work on supernova remnants, both theoretical and observational, most of which is described in a review by Chevalier (1977). A number of authors have carried out numerical studies of the evolution of such remnants with a wide variety of input physics (Rosenberg & Scheuer 1973; Straka 1974; Chevalier 1974a, b; Mansfield & Salpeter 1974). Although the fundamental theory of their evolution seems quite well established, there remain a number of discrepancies between theory and observation. In particular, the X-ray temperature of supernova remnants is always much higher than that behind a shock travelling with the expansion velocity of the optical filaments. This has led a number of authors (McKee & Cowie 1975; McKee, Cowie & Ostriker 1978; Lozinskaya 1978) to assume that the optical filaments are produced by dense clouds embedded in a much rarer medium. However, it is found here that, once radiative cooling has occurred, there need be no correlation between the velocity of the optical filaments and the X-ray temperature of the remnant.

It has been shown in a previous paper (Falle 1975; hereafter referred to as Paper I) that the onset of radiative cooling is sudden, and that additional shocks may be formed during the transition from the Sedov to the thin-shell phase. This transition has not been studied in detail by other authors, mainly because of the complexity of the flow during this phase, but a proper treatment is important for several reasons. First, most of the energy of the remnant is radiated away during this phase and so to a large extent it determines the subsequent evolution of the remnant. Secondly, Bell (1978) and Blandford & Ostriker (1978)

have suggested that cosmic rays are accelerated by supernova shocks. The number and strength of the additional shocks can then have an important effect on the cosmic rays produced by a supernova remnant.

For these reasons we will consider the rapid cooling phase of supernova remnants in some detail, using the numerical code described in Paper I. This treats shocks by shock-fitting and readily allows a variable mesh-spacing to cope with locally steep gradients. The problem of rapid cooling is thus treated more satisfactorily than by other methods, although the formation of multiple shocks clearly causes some programming difficulties.

The physical assumptions are described in Section 2 together with a brief description of the numerical code used. From the equations given in Section 2, the appropriate scaling laws are derived in Section 3. These are then used in Section 4 to derive the time at which radiative cooling becomes important. A criterion for the formation of secondary shocks is derived in Section 5, while the numerical results are presented in Section 6.

2 Physical assumptions and computational method

The physical assumptions are broadly the same as in Paper I, namely:

(i) The flow is initially described by the Sedov solution for a uniform medium with $\gamma = 5/3$. This assumes that the time t_b at which the remnant enters the Sedov phase is less than the time t_{sg} at which radiative cooling becomes important.

In Paper I it was shown that

$$t_b < 7\times10^3\left(\frac{M_e}{M_\odot}\right)^{5/6}\left(\frac{E_0}{10^{51}}\right)^{-1/2} n_0^{-1/3}\ \text{yr}, \tag{2.1}$$

where M_e is the mass ejected during the explosion, E_0 is the explosion energy and n_0 is the interstellar number density. It will be shown in Section 4 that

$$t_{sg} = 2.7\times10^4\left(\frac{E_0}{10^{51}}\right)^{0.24} n_0^{-0.52}\ \text{yr}. \tag{2.2}$$

The requirement that a Sedov phase exists then becomes

$$\frac{t_b}{t_{sg}} = 0.26\left(\frac{E_0}{10^{51}}\right)^{-0.74}\left(\frac{M_e}{M_\odot}\right)^{5/6} n_0^{0.19} < 1. \tag{2.3}$$

This is satisfied for all cases considered in this paper, provided that $M_e \lesssim M_\odot$.

(ii) The magnetic field is tangential everywhere and is a function of radius only, i.e.

$$\mathbf{B} = [0, 0, B(r)] \tag{2.4}$$

in spherical polars. The magnetic field does not become dynamically important until the gas has cooled and the resulting compression has amplified the field. Although unphysical, (2.4) will then be a reasonable approximation since only the tangential component of the field is magnified.

(iii) The cooling rate per unit volume is

$$L = n_H n_e \Phi(T) \qquad \text{erg cm}^{-3}\,\text{s}^{-1}, \tag{2.5}$$

where n_H, n_e are the hydrogen and electron number densities respectively. For $T \geqslant 10^6$K, $\Phi(T)$ is taken from Cox & Daltabuit's (1971) calculations for an optically thin gas with

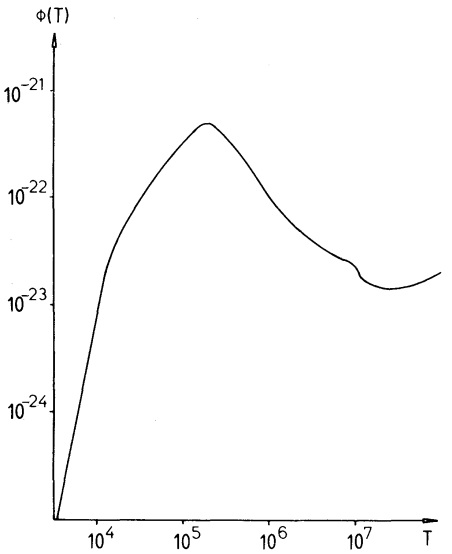

Figure 1. Cooling law (Kafatos 1973).

Aller's (1961) abundances. In the range $10^4\,\mathrm{K} \leqslant T \leqslant 10^6\,\mathrm{K}$, $\Phi(T)$ is taken from Kafatos' (1973) calculations which take into account the fact that in this temperature range the gas cools too rapidly to stay in ionizational equilibrium. For $T < 10^4\,\mathrm{K}$ the cooling is complicated by the fact that the hydrogen recombines and the gas becomes optically thick to radiation beyond the Lyman limit. However, when the gas cools to these temperatures, the magnetic pressure exceeds the gas pressure so that the dynamics are independent of the cooling law for $T < 10^4\,\mathrm{K}$. As in Paper I we therefore assume $\Phi \propto T^4$ for $T < 10^4\,\mathrm{K}$. The function $\Phi(T)$ is shown in Fig. 1.

(iv) The thermal conductivity of the gas is neglected. Several authors (Chevalier 1975; Solinger, Rappaport & Buff 1975) have considered the effect of thermal conduction and Chevalier has shown that it makes the interior of the remnant isothermal. These authors assume that the thermal conductivity is

$$K = 10^{-6} T^{5/2}, \tag{2.6}$$

which is valid for a fully ionized hydrogen gas if there is no magnetic field. In the presence of a field, however, the thermal conductivity parallel to the field is unchanged, but that perpendicular to the field becomes

$$K_\perp = 5.5 \times 10^{-16} \frac{n_{\mathrm{H}}^2}{B^2 T^{1/2}}. \tag{2.7}$$

Thermal conduction is only important at temperatures above $10^6\,\mathrm{K}$, and $K_\perp$ will then be less than K if $B \geqslant 10^{-14}\,\mathrm{G}$ (for $n_{\mathrm{H}} = 1$). The magnetic field is certainly much greater than this, except near the centre of the remnant where the density is very low. If there is turbulence with an energy density greater than the field energy density then the field will become random and prevent conduction. Near the shell, the turbulent energy density is a few percent of the thermal energy density and thus always greater than the field energy density. In the interior of the remnant, this turbulence will have decayed and the field will be more ordered. Conduction may then be important in the interior, unless there are inhomogeneities which can generate turbulence. But since most of the energy is near the shock, conduction in the interior will not have an important effect on the remnant. In

particular, it will not alter the energetics of those regions which are cooling radiatively, since these are near the shock.

(v) The ambient gas is uniform, fully ionized, at a temperature of 10^4K and is at rest. Any motions in the ambient medium will be of the order of the sound speed and so may be neglected as long as the shock is strong.

Kahn (1974) has shown that, for a supernova explosion with a total energy of 10^{52}erg, the amount in ionizing radiation is $\sim 10^{47}$erg. At a density of one hydrogen atom cm^{-3}, this can only ionize a sphere ~ 5 pc in radius, even without allowing for recombinations. The ambient gas cannot therefore be ionized by the original explosion, although Cox (1972a) has shown that, if the shock velocity is greater than ~ 50 km s^{-1}, the radiation from the gas cooling behind the shock can ionize the gas ahead.

As to the assumption of uniform density, this is clearly invalid for most supernova remnants. While there would clearly be no difficulty in considering the ambient density to be a function of radius, the most interesting effects would be produced by non-spherically symmetric density distributions. Since these cannot be studied with a spherically symmetric code, we adopt a uniform density for simplicity.

With a magnetic field of the form (2.4) and spherical symmetry, the hydrodynamic equations for a perfectly conducting gas are,

$$\rho\left(\frac{\partial u}{\partial t}+u\frac{\partial u}{\partial r}\right)=-\frac{\partial p}{\partial r}-\frac{\partial}{\partial r}\frac{B^2}{8\pi}-\frac{B^2}{4\pi r} \quad \text{(momentum)}, \tag{2.8}$$

$$\frac{\partial B}{\partial t}=-\frac{\partial}{\partial r}uB-\frac{uB}{r} \quad \text{(flux conservation)}, \tag{2.9}$$

$$\frac{\partial \rho}{\partial t}+\frac{\partial}{\partial r}\rho u+\frac{2\rho u}{r}=0 \quad \text{(continuity)}, \tag{2.10}$$

$$\frac{\partial p}{\partial t}+u\frac{\partial p}{\partial r}-\frac{\gamma p}{\rho}\left(\frac{\partial \rho}{\partial t}+u\frac{\partial \rho}{\partial r}\right)+(\gamma-1)L=0 \quad \text{(energy)}, \tag{2.11}$$

$$p=\frac{k\rho T}{\mu m_{\mathrm{H}}} \quad \text{(state)}. \tag{2.12}$$

Here μ (= 0.66) is the mean molecular weight.

In addition to equations (2.8) to (2.12) we have the Rankine–Hugoniot conditions at the shock which bounds the remnant,

$$\rho(V-u)=\rho_0 V, \tag{2.13}$$

$$\frac{B^2}{8\pi}+p+\rho(V-u)^2=\frac{B_0^2}{8\pi}+p_0+\rho_0 V^2, \tag{2.14}$$

$$\frac{B^2}{4\pi\rho}+\frac{\gamma}{(\gamma-1)}\frac{p}{\rho}+\frac{1}{2}\rho(V-u)^2=\frac{B_0^2}{4\pi\rho_0}+\frac{\gamma p_0}{(\gamma-1)\rho_0}+\frac{1}{2}\rho V^2. \tag{2.15}$$

Here V is the velocity of the shock in a fixed frame, and ρ_0, p_0 and B_0 are the ambient density, pressure and magnetic field respectively.

In Paper I it was shown that (2.8) to (2.12) could be transformed into differential relations along the characteristics. The method used to integrate these equations is described in Paper I. Shocks are treated by shock-fitting unless they are very weak, in which case they are handled satisfactorily by the small artificial viscosity introduced by the way in which the

equations are differenced. Additional shocks are formed during the evolution of the remnant, and this leads to shocks overtaking each other. The method for dealing with this is described in the Appendix.

The scheme is explicit and correct to second order. Stability requires that the time-step be limited by the Courant–Friedrichs condition, except when cooling becomes so rapid that the cooling time is shorter than the Courant–Friedrichs time. In order to handle the steep gradients which occur, it is necessary to use different mesh-spacings in different parts of the flow. There were usually six to nine different regions and, since the permissible time-step varies by several orders of magnitude across the remnant, different time-steps were used in each of these regions.

Note that if the shocks are treated by artificial viscosity, then the cooling time must be greater than the Courant–Friedrichs time at the shock. Otherwise a gas element will cool significantly in passing through the finite thickness of the shock and, since the shock structure produced by artificial viscosity is incorrect, the energy radiated by the gas element will be incorrect. We shall see in Section 6 that a significant fraction of the energy of the remnant is radiated away near secondary shocks, for which the cooling time would be shorter than the Courant–Friedrichs time unless an unacceptably small mesh-spacing were used. This means that it is extremely difficult to calculate the energy of a supernova remnant accurately if artificial viscosity is used.

It can of course be argued that the simplifying assumptions used in the present work cause errors as large as those introduced by the use of artificial viscosity. However, if artificial viscosity is used, and the cooling time is shorter than the Courant–Friedrichs time, then gas passing through a shock is not heated to a high temperature. As we shall see later, the cooling of gas from a high temperature produces interesting dynamical effects, which depend only on certain gross features of the cooling law. These effects would be lost if artificial viscosity were used.

3 Scaling laws

The cooling law (2.5) can be written in the form

$$L = A\rho^2\phi\left(\frac{c}{c_*}\right), \tag{3.1}$$

where ϕ is a dimensionless function and

$$c = \frac{\gamma p}{\rho} \tag{3.2}$$

is the sound speed in the gas. c_* is a reference sound speed which we take to be that at the maximum of the cooling curve. Then

$$c_* = \left(\frac{\gamma k T_*}{\mu m_{\mathrm{H}}}\right)^{1/2} = 6.09 \times 10^6, \tag{3.3}$$

where T_* is the temperature at the maximum of the cooling curve. If we choose $\phi(1) = 1$ we get

$$A = 1.88 \times 10^{26}. \tag{3.4}$$

For a given function ϕ, the flow is governed by the parameters E_0, ρ_0, A, c_*, B_0 and c_0, where B_0 and c_0 are the ambient magnetic field and sound speed respectively. From these

we can construct three dimensionless parameters which we choose to be

$$\mathscr{A} = \frac{E_0 \rho_0^2}{c_*^{11}} A^3, \qquad \mathscr{B} = \frac{\gamma B_0^2}{\gamma \pi \rho_0 c_*^2}, \qquad \mathscr{C} = \frac{c_0}{c_*}. \tag{3.5}$$

We shall see later that the magnetic field is only important when the gas has cooled substantially, so that until this happens the flow cannot depend on $\mathscr{B}$. The parameter $\mathscr{C}$ will only have an effect at the very latest times when the shock is no longer strong. We can thus divide the flow into three stages. In the first the magnetic field is unimportant and the flow depends only on $\mathscr{A}$; in the second it depends on both $\mathscr{A}$ and $\mathscr{B}$; while in the third it depends on all three. The time at which the first stage ends depends on $\mathscr{B}$, and the time at which the second ends depends on $\mathscr{C}$.

In view of this it is convenient to choose characteristic mass m_c, length ℓ_c and time t_c which do not involve B_0 and c_0. A suitable choice is

$$m_c = \frac{E_0}{c_*^2}, \qquad \ell_c = \left(\frac{E_0}{\rho_0 c_*^2}\right)^{1/3}, \qquad t_c = \left(\frac{E_0}{\rho_0 c_*^5}\right)^{1/3}. \tag{3.6}$$

All solutions with the same values of $\mathscr{A}$, $\mathscr{B}$ and $\mathscr{C}$ can be obtained from each other using this scaling-law. Furthermore, in the first stage of the flow the solutions need only have the same values of $\mathscr{A}$, and in the second the same values of $\mathscr{A}$ and $\mathscr{B}$.

For galactic supernovae we would expect $10^{50} \leqslant E_0 \leqslant 10^{52}$, $10^{-1} \leqslant n_0 \leqslant 10$, $10^{-7} \leqslant B_0 \leqslant 10^{-5}$. The possible range for the ambient temperature T_0 is 100 K $\leqslant T_0 \leqslant 10^6$ K, but we shall only consider $T_0 = 10^4$ K. The dimensionless parameters $\mathscr{A}$, $\mathscr{B}$ and $\mathscr{C}$ then lie in the ranges $4.3 \times 10^6 \leqslant \mathscr{A} \leqslant 4.3 \times 10^{10}$, $10^{-6} \leqslant \mathscr{B} \leqslant 1$ and $\mathscr{C} = 0.24$.

4 Onset of radiative cooling

The considerations of the last section can immediately be used to obtain an expression for the time at which radiative cooling becomes important. In the Sedov solution the temperature gradient behind the shock is negative, so that the magnetic field cannot be important unless it is so behind the shock. However, the field is negligible behind a strong adiabatic shock unless it dominates ahead of the shock. Since we shall not consider such cases, we can be certain that the flow is unaffected by the field and hence does not depend on $\mathscr{B}$ until radiative cooling becomes important. Once this happens, the temperature gradient behind the shock will increase, so, following Cox (1972b), we will define t_{sg} as the time at which the temperature gradient behind the shock vanishes. This gives a good indication of the time at which radiative cooling becomes significant. This time t_{sg} must be independent of $\mathscr{B}$ and $\mathscr{C}$.

We have on dimensional grounds

$$t_{sg} = t_c f(\mathscr{A}). \tag{4.1}$$

The dimensionless function $f(\mathscr{A})$ is found by computing t_{sg} for a number of values of $\mathscr{A}$. For $\mathscr{A}$ in the range given in Section 3, we find

$$f(\mathscr{A}) = 1.06 \times 10^{-1} \mathscr{A}^{-7/75}. \tag{4.2}$$

Putting this into (4.1), and substituting for $\mathscr{A}$ and t_c from (3.5) and (3.6), we get

$$t_{sg} = 1.06 \frac{E_0^{0.24}}{c_*^{0.64} A^{0.28} \rho_0^{0.52}}. \tag{4.3}$$

For the adopted values of A and c_* this gives

$$t_{sg} = 2.7 \times 10^4 \left(\frac{E_0}{10^{51}}\right)^{0.24} n_0^{-0.52} \text{ yr}. \tag{4.4}$$

Similarly we find that the shock velocity and radius at this time are given by

$$V_{sg} = 1.72 \frac{\ell_c}{\ell_c} \mathscr{A}^{0.0554}, \tag{4.5}$$

$$R_{sg} = 0.476 \ell_c \mathscr{A}^{-0.038}. \tag{4.6}$$

These become

$$V_{sg} = 2.77 \times 10^2 \left(\frac{E_0}{10^{51}} n_0^2\right)^{0.0554} \text{ km s}^{-1}, \tag{4.7}$$

$$R_{sg} = 2.0 \times 10^1 \left(\frac{E_0}{10^{51}}\right)^{0.295} n_0^{-0.409} \text{ pc}. \tag{4.8}$$

As can be seen from Figs 2 and 3, the shock velocity and radius at this time are little different from those for the Sedov solution. Because of this, (4.7) and (4.8) are nearly the

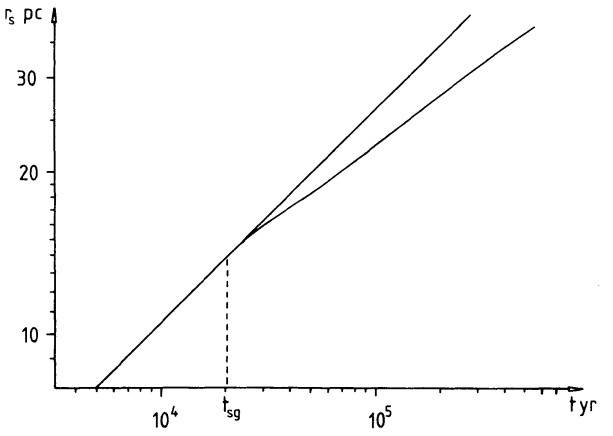

Figure 2. Shock radius r_s as a function of time. The straight line is the Sedov solution.

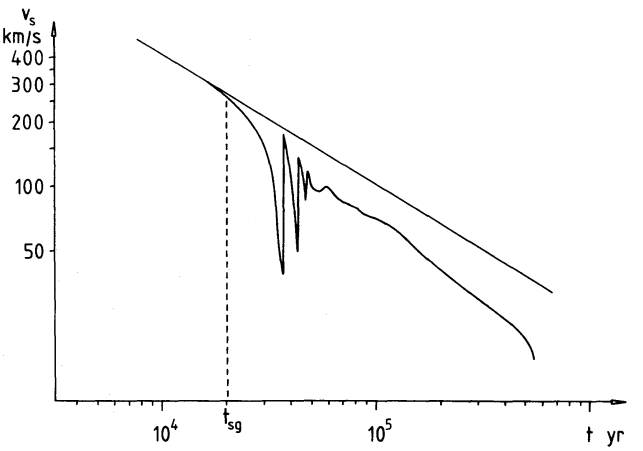

Figure 3. Shock velocity v_s as a function of time. The straight line is the Sedov solution.

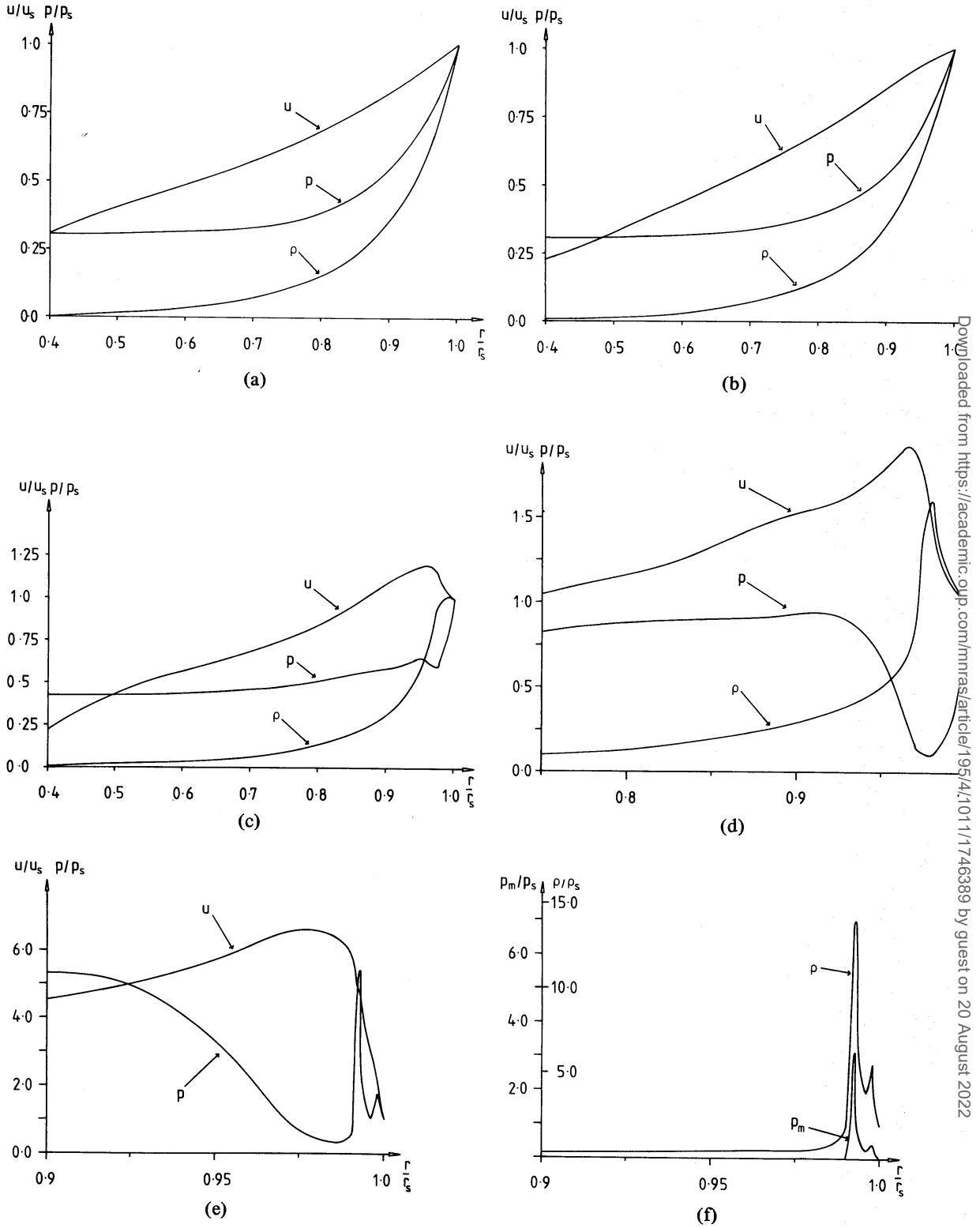

Figure 4. Flow at various times. u_s, p_s and ρ_s are the post-shock values. (a) Sedov solution for $\gamma = 5/3$. (b) $t = 2.10$ yr, $r_s = 14.1$ pc, $u_s = 1.90 \times 10^2$ km s^{-1}, $p_s = 8.14 \times 10^{-10}$ dyn cm^{-2}, $\rho_s = 6.60 \times 10^{-24}$ g cm^{-3}. (c) $t = 2.93 \times 10^4$ yr, $r_s = 15.9$ pc, $u_s = 1.31 \times 10^2$ km s^{-1}, $p_s = 3.90 \times 10^{-10}$ dyn cm^{-2}, $p_s = 6.50 \times 10^{-24}$ g cm^{-3}. (d) $t = 3.21 \times 10^4$ yr, $r_s = 16.4$ pc, $u_s = 9.28 \times 10^1$ km s^{-1}, $p_s = 1.98 \times 10^{-10}$ dyn cm^{-2}, $\rho_s = 6.34 \times 10^{-24}$ g cm^{-3}. (e) $t = 3.56 \times 10^4$ yr, $r_s = 16.7$ pc, $u_s = 2.97 \times 10^1$ km s^{-1}, $p_s = 2.55 \times 10^{-11}$ dyn cm^{-2}, $\rho_s = 4.76 \times 10^{-24}$ g cm^{-3}. (f) $t = 3.56 \times 10^4$ yr. (g) $t = 3.70 \times 10^4$ yr, $r_s = 16.8$ pc, $u_s = 1.27 \times 10^2$ km s^{-1}, $p_s = 3.68 \times 10^{-10}$ dyn cm^{-2}, $p_s = 6.50 \times 10^{-24}$ g cm^{-3}. (h) $t = 9.01 \times 10^4$ yr, $r_s = 22.0$ pc, $u_s = 5.22 \times 10^1$ km s^{-1}, $p_s = 6.67 \times 10^{-11}$ dyn cm^{-2}, $p_s = 5.77 \times 10^{-24}$ g cm^{-3}. (i) $t = 9.01 \times 10^4$ yr.

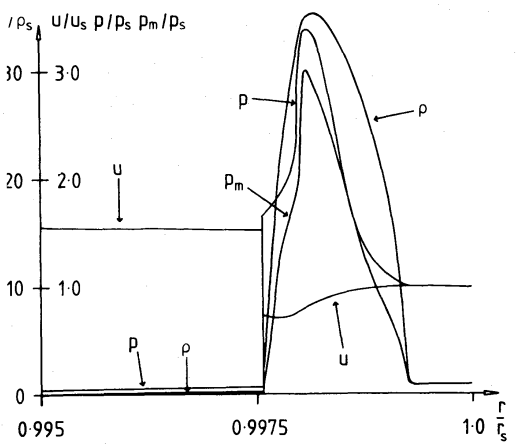

(g)

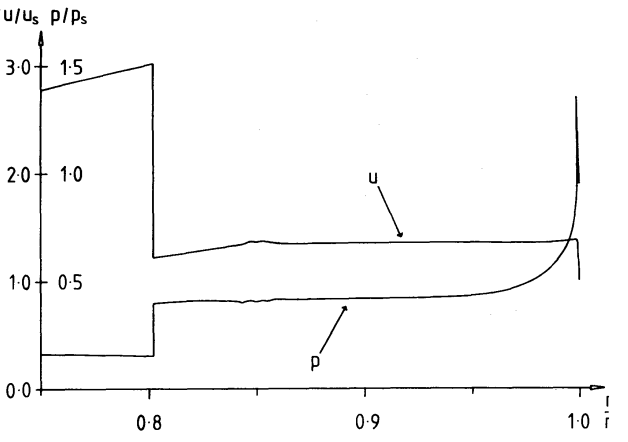

(h)

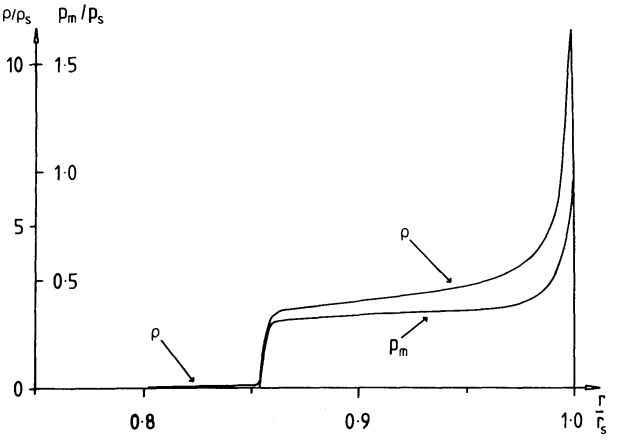

(i)

Figure 4 – *continued*

same as the expressions obtained by substituting t_{sg} into the Sedov solution. The structure of the flow behind the shock has, however, changed significantly. This can be seen in Fig. 4(b).

The post-shock temperature at $t = t_{sg}$ is given by

$$T_{sg} = 1.5 \times 10^{-9} V_{sg}^2 = 4.41 \times 10^{-9} \frac{\ell_c^2}{\ell_c^2} \mathscr{A}^{0.1108}. \tag{4.9}$$

This is

$$T_{sg} = 1.15 \times 10^6 \left(\frac{E_0 n_0^2}{10^{51}}\right)^{0.1108} \text{K}. \tag{4.10}$$

For the range of $E_0 n_0^2$ considered, T_{sg} lies in the range

$$5.3 \times 10^5 \text{K} \leqslant T_{sg} \leqslant 2.5 \times 10^6 \text{K}. \tag{4.11}$$

In the temperature range

$$T_* = 1.78 \times 10^5 \text{K} \leqslant T \leqslant 3 \times 10^6 \text{K}, \tag{4.12}$$

the cooling function ϕ is approximately a power-law, and this, together with the fact that cooling only becomes important when $t \simeq t_{sg}$, is the reason why $f(\mathscr{A})$ is a power-law. We also find that, as long as the temperature in the remnant is everywhere greater than T_*, then radiative cooling is only important in regions where the temperature is in the range defined by (4.12). This allows us to deduce an approximate scaling-law which is valid as long as the temperatue is greater than T_* throughout the remnant.

If the cooling law has the form

$$L = B\rho^2\left(\frac{p}{\rho}\right)^{\alpha}, \tag{4.13}$$

then the characteristic mass m'_c, length l'_c and time t'_c are given by

$$\begin{aligned} m'_c &= E_0^{3(2\alpha-3)/(6\alpha-11)}\rho_0^{4/(6\alpha-11)}B^{2/(6\alpha-11)}, \\ l'_c &= E_0^{(2\alpha-3)/(6\alpha-11)}\rho_0^{(5-2\alpha)/(6\alpha-11)}B^{2/(6\alpha-11)}, \\ t'_c &= E_0^{2(\alpha-1)/(6\alpha-11)}\rho_0^{(7-2\alpha)/(6\alpha-11)}B^{5/(6\alpha-11)}. \end{aligned} \tag{4.14}$$

(4.3) then shows that we must have

$$\alpha = -1.14. \tag{4.15}$$

The approximate scaling-law (4.14) then becomes

$$\begin{aligned} m'_c &= E_0^{0.888}\rho_0^{-0.224}B^{-0.336}, \\ l'_c &= E_0^{0.296}\rho_0^{-0.408}B^{-0.112}, \\ t'_c &= E_0^{0.24}\rho_0^{-0.52}B^{-0.28}. \end{aligned} \tag{4.16}$$

As long as ϕ can be approximated by a power-law, the flow does not depend on any dimensionless parameter. The scaling-law (4.16) can then be used to obtain the solution for any value of the parameters from a single computation.

This scaling breaks down when the temperature falls below T_*. From the computations, we find that this occurs at $t = t_1$ with

$$t_1 = 4.06 \times 10^4 \left(\frac{E_0}{10^{51}}\right)^{0.24} n_0^{-0.52} \text{ yr}. \tag{4.17}$$

For $t < t_1$, solutions may be scaled according to (4.16). We shall make use of this fact in the next section.

As far as scaling is concerned, we can thus divide the evolution of the remnant into four stages. In the first up to $t = t_1$, the scaling-law (4.16) holds and the flow does not depend on any dimensionless parameters. In the second, from $t = t_1$ to $t = t_2$, say, the flow depends only on $\mathscr{A}$. We shall see later that this stage is very short, so that $t_2 \simeq t_1$. From $t = t_2$ to $t = t_3$ the flow depends only on $\mathscr{A}$ and $\mathscr{B}$, while for $t > t_3$ it depends on all three parameters. Note that, while t_1 is independent of $\mathscr{A}$, $\mathscr{B}$ and $\mathscr{C}$, t_2 depends on $\mathscr{A}$ and $\mathscr{B}$, and t_3 depends on $\mathscr{A}$, $\mathscr{B}$ and $\mathscr{C}$. t_1 is precisely defined, whilst t_2 and t_3 are somewhat vaguely defined since they depend on the definition of a small effect of $\mathscr{B}$ and $\mathscr{C}$ on the flow.

5 Conditions for the formation of additional shocks

It was shown in Paper I that, if $E_0\rho_0^2$ was sufficiently large, then the radiative cooling was so rapid that additional shocks were formed. In this section we will devise a condition on the form of the cooling-law and on $E_0\rho_0^2$ (i.e. on $\mathscr{A}$) for this to occur.

The local cooling time in the gas is

$$t_{\rm cool} = \frac{p}{(\gamma-1)L} = \frac{c^2}{\gamma(\gamma-1)} A\rho\phi(c^2/c_*^2) \tag{5.1}$$

from (3.1). If we assume that the region in which radiative cooling is important originally has size λ_i, mean sound speed $\bar{c}_i$ and mean density $\bar{\rho}_i$, then continuity gives

$$\frac{\lambda}{\lambda_i} = \frac{\bar{\rho}_i}{\bar{\rho}}. \tag{5.2}$$

Here $\bar{\rho}$ and λ are the mean density and size of the region at any later time. We have assumed that the cooling region is thin so that it may be regarded as approximately plane parallel, and that the radius does not change significantly.

The sound crossing-time in this region is then

$$t_s = \frac{\lambda}{\bar{c}} = \frac{\bar{\rho}_i \lambda_i}{\bar{\rho}\bar{c}}, \tag{5.3}$$

where $\bar{c}$ is the mean sound speed in this region. We expect additional shocks to be formed if $t_{\rm cool} < t_s$ at any time. The ratio of these times is

$$\frac{t_{\rm cool}}{t_s} = \frac{\bar{c}^3}{\gamma(\gamma-1)A\phi(\bar{c}^2/c_*^2)\rho_i\lambda_i}. \tag{5.4}$$

As the gas cools, $\bar{c}$ decreases, and so the ratio of these times will decrease if

$$\frac{d}{d\bar{c}} \frac{\bar{c}^3}{\phi(\bar{c}^2/c_*^2)} > 0. \tag{5.5}$$

If

$$\phi\left(\frac{\bar{c}^2}{c_*^2}\right) \propto \left(\frac{\bar{c}^2}{c_*^2}\right)^{\alpha}, \tag{5.6}$$

then this requires

$$\alpha < \frac{3}{2}. \tag{5.7}$$

Note that this is a stricter requirement than the condition for the thermal instability during isobaric cooling, which merely requires $\alpha < 3$ (McCray, Stein & Kafatos 1975).

Additional shocks will not form unless $t_{\rm cool}/t_s$ becomes less than unity. We then require

$$\left(\frac{t_{\rm cool}}{t_s}\right)_{\rm min} = \frac{[\bar{c}^3/\phi(\bar{c}^2/c_*^2)]_{\rm min}}{\gamma(\gamma-1)A\rho_i\lambda_i} < 1, \tag{5.8}$$

where $[\bar{c}^3/\phi(\bar{c}^2/c_*^2)]_{\rm min}$ is the minimum value. This is simply a property of the cooling law, and for the law which we have adopted we find

$$\left[\frac{\bar{c}^3}{\phi(\bar{c}^2/c_*^2)}\right]_{\rm min} = 9.75 \times 10^{19} \tag{5.9}$$

at $\bar{c} = 2.57 \times 10^6$ ($T = 3.16 \times 10^4$ K).

Clearly λ_i and ρ_i are somewhat uncertain, but it is reasonable to take ρ_i to be simply the adiabatic post-shock density,

$$\rho_i = \left(\frac{\gamma+1}{\gamma-1}\right)\rho_0. \tag{5.10}$$

We will take the cooling region to be the gas swept up between t_{sg} and the onset of rapid cooling. The latter can be defined as the time when the pressure gradient begins to depart from that in the Sedov phase. Since $T > T_*$ everywhere up to this point, we can use the approximate scaling-law (4.16). We then have

$$\lambda_i \propto \frac{E_0^{0.296}}{\rho_0^{0.408}}.$$

From a single computation we find

$$\lambda_i = 3.5\times10^{-7}\frac{E_0^{0.296}}{\rho_0^{0.408}}. \tag{5.11}$$

Substituting (5.9), (5.10) and (5.11) into condition (5.8), we get

$$\frac{E_0 n_0^2}{10^{51}} > 8.8\times10^{-6}. \tag{5.12}$$

In Paper I it was shown by computation that the condition is

$$\frac{E_0 n_0^2}{10^{51}} > 2.7\times10^{-5}. \tag{5.13}$$

Given the crudity of the assumptions used to derive (5.12), the agreement is quite satisfactory.

In terms of the parameter $\mathscr{A}$, (5.13) becomes

$$\mathscr{A} > 1.15\times10^3, \tag{5.14}$$

which is satisfied for almost all supernova remnants.

The arguments of this section can be applied to any flow in which the cooling law satisfies (5.5) at any point. In particular, they have been applied by Dyson, Falle & Perry (1980) to the flow resulting from the interaction of a QSO wind with ambient material.

6 Numerical results

Since we are primarily concerned with studying the shocks produced by rapid cooling, we will restrict ourselves to supernova remnants with $\mathscr{A} > 1.15\times10^3$. In order that the present work may be compared with Chevalier's (1975) results, we choose $E_0 = 3\times10^{50}$ erg, $\rho_0 = 1.67\times10^{-24}$ g cm^{-3}, $B_0 = 10^{-6}$ G. This gives $\mathscr{A} = 1.3\times10^7$, $\mathscr{B} = 6.42\times10^{-4}$ and $\mathscr{C} = 0.24$. These values correspond to Chevalier's model A except that he uses a field of 3×10^{-6} G. In fact we find that the field has little effect on the overall flow unless the magnetic pressure becomes important in regions in which the temperature is greater than T_*. Note, however, that for values of $\mathscr{A}$ such that additional shocks form, it is necessary to use a finite value of B_0. Otherwise the density becomes very high and the consequent decrease in the Courant–Friedrichs time makes it impossible to continue the computations.

For this model we have from (4.4)–(4.6) $t_{sg} = 2.02 \times 10^4$ yr, $R_{sg} = 13.99\,\rho c$, $V_{sg} = 2.59 \times 10^2$ km s^{-1}. These values are marked on Figs 2 and 3. The structure of the remnant is shown in Fig. 4. The flow variables are plotted as functions of the Eulerian radius, in contrast to Paper I where they were shown as functions of the Lagrangian variable $m(r)$ which is the mass interior to radius r. Although this makes a physical interpretation of the results easier, the considerable compression which occurs makes it necessary to show only a part of the flow in the later stages.

Fig. 4(a)–(d) correspond roughly to Fig. 5(a)–(d) in Paper I and show that cooling sets in suddenly, so that a low-pressure region is formed behind the shock. This is because, as expected for this value of $\mathscr{A}$, the cooling time in this region becomes shorter than the sound crossing-time.

The flow during the period of thin-shell formation is shown schematically in Fig. 5, while the corresponding numerical results are shown in Fig. 4(d)–(i). In Fig. 5(a) the low-pressure region is idealized as being bounded by pressure discontinuities. The break-up of these discontinuities is shown in Fig. 5(b). s_2 and s_3 are shocks which move into the low-pressure region, while R_1 and R_2 are rarefaction waves moving away from this region. For this value of $\mathscr{A}$, s_2 and s_3 are weak and can be handled by the small artificial viscosity inherent in the numerical code whereas, for larger values of $\mathscr{A}$, the shocks are strong and must be treated by shock fitting. The temperature behind s_2 and s_3 remains low because of the short cooling-time. Contact discontinuities are not shown since they disappear in a cooling-time. s_2 and s_3 collide and produce two much stronger shocks s_4 and s_5 as shown in Fig. 5(c). This corresponds to Fig. 4(e) and (f) and it can be seen that the cooling time behind s_4 and s_5 is short. In Fig. 5(d), which corresponds to Fig. 4(g), s_5 has overtaken s_1, causing it to accelerate and producing an inward-moving rarefaction wave R_3. This rarefaction eventually overtakes s_4 and weakens it somewhat.

Once s_1 has been overtaken by s_5, the temperature in the gas behind it exceeds T_*, so that it is once more subject to the catastrophic cooling described in Section 5. A low-pressure region is again formed behind s_1 and the whole process repeats itself. In Fig. 2 it can be seen that this process of shock formation occurs four times in all. In fact, the process only ceases when s_1 is no longer accelerated to a velocity greater than 108 km s^{-1}, which is the shock speed at which the post-shock temperature is equal to T_*. As shown in Section 5, gas cooling from a temperature less than T_* can cool in approximate pressure equilibrium so that additional shocks are not formed. For larger values of $\mathscr{A}$, the process repeats itself more times and again only ceases when s_1 is no longer accelerated to velocities greater than 108 km s^{-1}.

During this process, the cooling time behind s_1 is shorter than the Courant–Friedrichs time. Thus if artificial viscosity is used, the gas will not be heated to a high temperature by

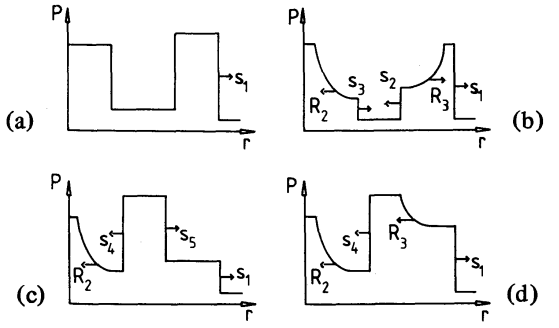

Figure 5. Schematic diagram of the flow showing the formation of additional shocks.

s_1. Repeated shock-formation would then either not occur, or the oscillations in shock strength would have much smaller amplitude.

Once the bulk of the gas has cooled, and the mean velocity of the cool material has fallen below 108 km s^{-1}, the flow is as in Fig. 4(h) and (i); 98 per cent of the mass of the remnant is in a cold shell whose thickness is 15 per cent of the radius. Throughout this shell, the magnetic pressure dominates over the gas pressure. This will be the case whatever the value of B_0, the only difference being that the cold shell will be thinner if B_0 is smaller.

The inner edge of the cold shell is bounded at $r/r_s = 0.85$ by a sharp transition in which gas cools rapidly from $\sim 10^5$ K down to $\sim 10^3$ K. As can be seen from the figure, the pressure and velocity are continuous across this region except for some small numerical oscillations. These are due to the large gradients. Inside this transition there is a region containing hot gas, which is bounded at $r/r_s = 0.8$ by the inward-moving shock s_4. Inside s_4 there is very hot gas ($T \geqslant 10^6$ K) which is expanding outwards. Radiative cooling is negligible in this gas because of the low density.

The outer edge of the cold shell is bounded by a very thin ($\Delta r/r_s = 0.01$) region in which the gas cools from the post-shock temperature of 8×10^4 K down to 10^3 K. It is this region which produces most of the optical emission from the remnant at this time. The spectrum of this radiation could be obtained by a calculation such as that performed by Cox (1972a) and Raymond (1976) for the cooling region behind a steady shock.

The remnant retains essentially this structure, with the cold shell gradually increasing in mass while s_4 weakens and eventually disappears. This continues until the velocity of the shell becomes less than 50 km s^{-1}. The radiation from the gas cooling behind the shock is then no longer able to ionize the ambient gas and so, unless the remnant is embedded in an H II region, the ionization structure in the cooling region will be complicated. The end result, however, will clearly be a slowly moving H I shell, whose thickness will depend on the ambient magnetic field.

The energy of the remnant is shown as a function of time in Fig. 6. Here E_I is the total energy input to the remnant and is given by

$$E_I = E_0 + \frac{4\pi}{3} r_s^3 \frac{\rho_0 c_0^2}{\gamma(\gamma - 1)}, \tag{6.1}$$

since the ambient gas has non-zero thermal energy. It can be seen that the bulk of the energy is radiated away during the period of additional shock formation from $t = 3.2 \times 10^4$ to

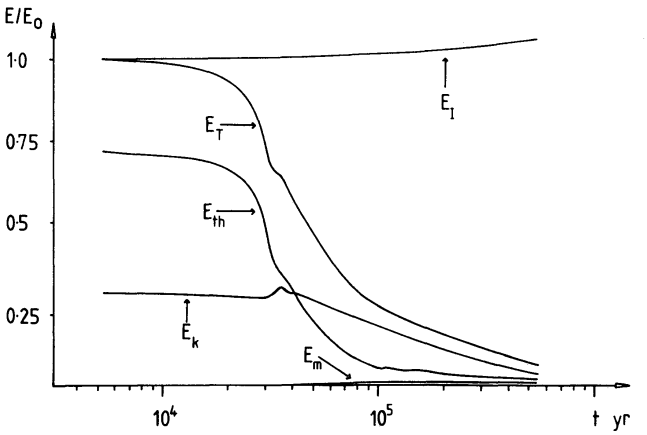

Figure 6. Energy of the remnant as a function of time. E_I is the total energy input, E_T the total energy of the remnant, E_{th} the thermal energy, E_k the kinetic energy and E_m the magnetic energy.

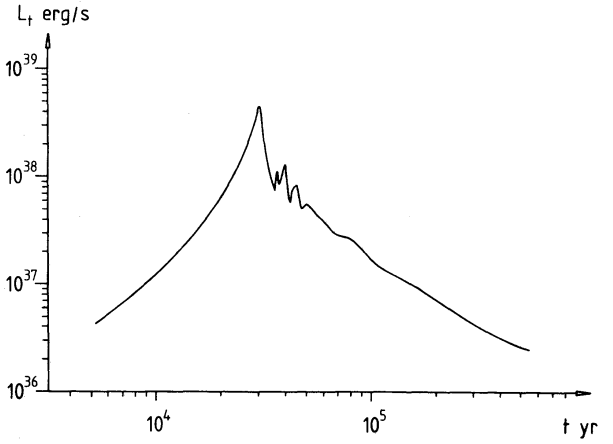

Figure 7. Total luminosity L_t as a function of time.

$t = 6.3 \times 10^4$yr. Note that the kinetic energy actually increases at one point due to the presence of rarefaction waves.

Fig. 7 shows the total luminosity of the remnant as a function of time. This is greatest during the first period of rapid cooling when the low-pressure region is first formed. Thereafter there are peaks associated with the formation of the additional low-pressure regions. A significant fraction of the luminosity at this time comes from gas cooling behind the additional shocks s_2 and s_3.

The X-ray luminosity in the band 1.5–4 keV is shown in Fig. 8. This was calculated using the results given by Tucker & Koren (1971) for a low-density plasma with solar abundances. The mean emission-weighted X-ray temperature is also shown in Fig. 8. It can be seen that this temperature correlates with the velocity of s_1 as long as radiative cooling is unimportant, but thereafter it actually increases while the velocity of s_1 decreases. This is because, once the thin shell has formed, the X-ray emission comes only from the hot interior and so does not depend on the velocity of the thin shell. This means that there is no discrepancy between the X-ray temperature measured for old remnants, such as the Cygnus Loop, and the expansion velocities of the optical filaments.

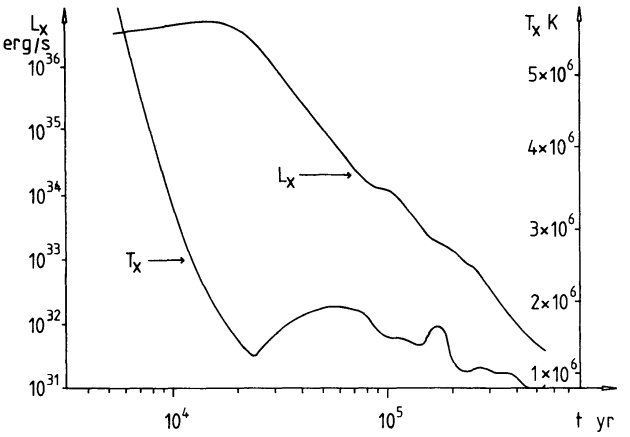

Figure 8. X-ray luminosity L_X in the band 1.5–4 keV and mean emission-weighted X-ray temperature T_X as functions of time.

7 Conclusion

The present paper extends the work described in Paper I in a number of ways. First, it has been shown in Section 3 that the scaling laws for supernova remnants can be simplified under certain circumstances. This allows more information to be obtained from the necessarily limited number of computations. The arguments leading to the criterion for the formation of additional shocks have also been improved in such a way as to make it easier to extend them to other situations.

The most important improvement, however, is that the additional shocks and their interactions are treated by shock-fitting. This has allowed the complete evolution of the remnant to be studied and has shown that additional shocks are formed many times. They are thus far more important than was supposed in Paper I. In particular they have a greater effect on the energetics of the remnant than had been thought. This means that the proper treatment of these shocks is even more crucial if the evolution of supernova remnants is to be correctly calculated.

It was pointed out in Section 2 that methods based on artificial viscosity, although suitable for many applications, are likely to lead to serious errors if used to treat these additional shocks. Although the method used in the present work overcomes most of the difficulties, it is very cumbersome when several shocks are involved. Clearly some more convenient way of handling these problems is needed.

The fact that even a simple one-dimensional problem presents such difficulties makes it difficult to trust two-dimensional calculations as at present performed. The coarse grid necessary for these calculations must lead to very large errors in the energy loss and hence distort the subsequent behaviour of the remnant. Their only value seems to be in carrying out model calculations for cases in which these limitations are not serious.

Finally, it has been shown that, once radiative cooling has occurred, there is no simple correlation between the X-ray temperature of the remnant and the expansion velocity of the thin shell. The high X-ray temperature of remnants such as the Cygnus Loop therefore provides no support for the idea that they are in the Sedov phase, the optical filaments being produced by shock interactions with denser clouds.

In the Cygnus Loop there have been observations of velocities corresponding to the X-ray temperature (Kirshner & Taylor 1976). It will be shown in a later paper that these, and other features of the Cygnus Loop, can be explained by a variation in the ambient density. The length-scale of this variation, however, appears to be of the same order as the size of the remnant, rather than much smaller as proposed by McKee & Cowie.

Acknowledgments

I thank Dr J. F. Scott for helpful discussions during the course of this work. The computations were carried out on the CDC7600 at the University of Manchester Regional Computing Centre. Part of this work was carried out while the author held a Royal Society European Exhange Fellowship.

References

Aller, L. H., 1961. *The Abundances of the Elements,* Interscience, New York.
Bell, A. R., 1978. *Mon. Not. R. astr. Soc.*, **182**, 147.
Blandford, R. D. & Ostriker, J. P., 1978. *Astrophys. J.*, **221**, L29.
Chevalier, R. A., 1974a. *Astrophys. J.*, **188**, 501.

Chevalier, R. A., 1974b. *Astrophys. J.*, **192**, 457.
Chevalier, R. A., 1975. *Astrophys. J.*, **198**, 355.
Chevalier, R. A., 1977. *A. Rev. Astr. Astrophys.*, **15**, 175.
Cox, D. P., 1972a. *Astrophys. J.*, **178**, 143.
Cox, D. P., 1972b. *Astrophys. J.*, **178**, 159.
Cox, D. P. & Daltabuit, E., 1971. *Astrophys. J.*, **167**, 47.
Dyson, J. E., Falle, S. A. E. G. & Perry, J. J., 1980. *Mon. Not. R. astr. Soc.*, **191**, 785.
Falle, S. A. E. G., 1975. *Mon. Not. R. astr. Soc.*, **172**, 55.
Kafatos, M., 1973. *Astrophys. J.*, **182**, 433.
Kahn, F. D., 1974. *IAU Symp. No. 60*, Reidel, Dordrecht, Holland.
Kirshner, R. P. & Taylor, K., 1976. *Astrophys. J.*, **208**, L83.
Lozinskaya, T. A., 1978. *Astr. Astrophys.*, **64**, 123.
McCray, R., Stein, R. F. & Kafatos, M., 1975. *Astrophys. J.*, **196**, 565.
McKee, C. F. & Cowie, L. L., 1975. *Astrophys. J.*, **195**, 715.
McKee, C. F., Cowie, L. L. & Ostriker, J. P., 1978. *Astrophys. J.*, **219**, L23.
Mansfield, V. N. & Salpeter, E. E., 1974. *Astrophys. J.*, **190**, 305.
Raymond, J. C., 1976. *PhD thesis*, University of Wisconsin.
Rosenberg, I. & Scheuer, P. A. G., 1973. *Mon. Not. R. astr. Soc.*, **161**, 27.
Solinger, A., Rappaport, S. & Buff, J., 1975. *Astrophys. J.*, **201**, 381.
Straka, W. C., 1974. *Astrophys. J.*, **190**, 59.
Tucker, W. H. & Koren, M., 1971. *Astrophys. J.*, **168**, 283.

Appendix

The computational method used when two shocks overtake each other is described in this Appendix. As long as the two shocks are separated by more than one mesh point, the integration can proceed as described in Paper I. Once they are only one mesh point apart, the situation will be as in Fig. A1. Here m is the Lagrangian variable, DE is the path of the

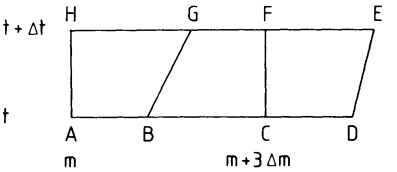

Figure A1

leading shock s_1 and BG is that of the trailing shock s_2 which is overtaking s_1. The mesh spacing is so chosen that the flow in region BCD changes little in the time it takes s_2 to overtake s_1. The flow between the shocks may then be regarded as steady, so that the flow variables ahead of s_2 can be obtained by interpolation on BCD. The flow in BCD is taken to be that obtaining when the situation of Fig. A1 first arises. In this way the solution can be advanced in time until the shocks are so close that they will intersect in the next time-step. This is shown in Fig. A2, where CE, DE are the paths of s_2 and s_1 respectively, and EF, EG

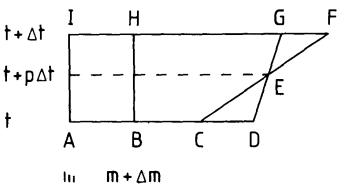

Figure A2

are the paths they would follow if they did not intersect at E. When the shocks intersect at E, a discontinuity is created, which breaks up into a rarefaction wave travelling to the left, a shock travelling to the right and a contact discontinuity at the point of intersection.

It is assumed that the flow is steady and plane parallel in the time interval $t + p\Delta t$ to $t + \Delta t$, so that the flow at $t + \Delta t$ can be found from the solution for a centred rarefaction wave and a plane steady shock. The solution can then be advanced as before, except that there is now a contact discontinuity at the value of the Lagrangian variable at which the shocks intersected. This can be treated just like an ordinary mesh point, except that there are two sets of equations along the streamlines, one on each side of the discontinuity.

In the present work, the gas ahead of s_1 is the undisturbed interstellar medium and so the flow there is known. However, it is not difficult to extend the method to cases in which the flow ahead of s_1 has to be obtained by computation.